Sensors and Materials, Vol. 38, No. 5 (2026) 2545–2556
MYU Tokyo

S & M 4452

Wind Turbine Gearbox Fault Detection Method Based on One-dimensional Convolutional Neural Network

Hong-Wei Sian*

Department of Electrical Engineering, National Chin-Yi University of Technology,
No. 57, Sec. 2, Zhongshan Rd., Taiping Dist., Taichung 411030, Taiwan (R.O.C.)

(Received May 23, 2025; accepted December 11, 2025)

Keywords: wind turbine, gearbox, one-dimensional convolutional neural network, fault detection, vibration signal

Wind turbines are often deployed in harsh and dynamic environments, rendering their gearboxes susceptible to unexpected faults that can result in significant downtime. Timely and accurate fault detection is therefore essential to ensure stable operation, minimize maintenance costs, and enhance overall system reliability. In this study, a fault detection framework for wind turbine gearboxes, which is based on a one-dimensional convolutional neural network (1D-CNN), is presented. Three representative fault conditions, including gear tooth breakage, gear tooth corrosion, and combined tooth breakage with corrosion, are constructed for evaluation. Triaxial vibration signals are collected using an accelerometer to capture critical operational features. The proposed 1D-CNN model is trained and tested using time-domain vibration data, enabling automated feature extraction and fault classification. Experimental results confirm the model's effectiveness in accurately identifying gearbox faults, demonstrating its potential for reliable health monitoring of wind turbine systems.

1. Introduction

With the increasing global demand for renewable energy, wind power has become one of the most rapidly expanding and widely implemented green energy sources.[1,2] In a wind turbine system, the gearbox has the vital role of transferring mechanical power from the rotor to the generator.[3,4] However, long-term operation under fluctuating environmental and mechanical conditions often induces gearbox failures, including gear wear, tooth corrosion, and bearing damage.[5–7] If not detected promptly, such faults may lead to unplanned shutdowns, costly maintenance, and even catastrophic system damage.

Most existing studies on gearbox fault diagnosis rely on analyzing vibration or operational data collected from the gearbox. Zhong *et al.* integrated an improved Hilbert–Huang transform with a pairwise-coupled sparse Bayesian extreme learning machine to enhance multifault identification accuracy.[8] Pu *et al.* proposed the deep enhanced fusion network, in which deep features extracted from triaxial vibration signals are fused and classified using an echo state

*Corresponding author: e-mail: hwsian@ncut.edu.tw
https://doi.org/10.18494/SAM5753

ISSN 0914-4935
https://myukk.org/

network.[9] He *et al.* introduced a multiview sparse filtering algorithm to autonomously learn representative features from raw current signals to enable unsupervised diagnosis.[10] Additionally, Xia *et al.* employed improved multivariate variational mode decomposition and multiscale entropy to enhance feature extraction for vibration-based fault classification.[11] Other researchers have explored data-driven approaches using supervisory control and data acquisition and machine learning models such as extreme gradient boosting to achieve efficient condition monitoring.[12] Although these methods exhibit good diagnostic performance, many depend on complex preprocessing or handcrafted features, which may limit accuracy and generalization when dealing with nonstationary signals or overlapping fault characteristics.

Recent advances in deep learning have significantly improved the capability of mechanical fault diagnosis, particularly through the use of one-dimensional convolutional neural networks (1D-CNNs).[13–16] By directly processing raw time-domain vibration signals, 1D-CNN models eliminate the need for manual feature engineering and reduce the information loss associated with two-dimensional signal transformations. In this study, a 1D-CNN-based gearbox fault detection framework is developed to enable the efficient and accurate classification of fault types. A triaxial accelerometer is installed on the gearbox to collect high-resolution vibration data during operation. Leveraging the advantages of 1D-CNN—such as local feature extraction, parameter sharing, and translational invariance—the model autonomously learns discriminative features from raw signals and effectively identifies different gearbox fault conditions. Experimental results show that the proposed method achieves a fault detection accuracy of 98.7%. To further assess its diagnostic capability, the vibration signals were also converted into chaotic scatter plots and classified using a two-dimensional convolutional neural network (2D-CNN),[17] as well as the histograms of oriented gradient (HOG)-based classical classifiers including the support vector machine (SVM), back-propagation neural network (BPNN), and k-nearest neighbor (KNN). The proposed method consistently outperforms traditional approaches in accuracy, computational efficiency, and overall diagnostic robustness, demonstrating its strong potential for real-time fault detection in wind turbine gearboxes.

2. Experimental Platform and Fault Modeling of Wind Turbine Gearbox

Wind turbine gearboxes are highly susceptible to failures due to long-term exposure to harsh environments such as high temperatures, humidity, and salt-induced corrosion. To analyze the vibration characteristics associated with typical fault conditions, a laboratory-scale experimental platform was developed to reproduce realistic operating scenarios and acquire high-quality diagnostic data. In collaboration with a professional gear manufacturer, three representative fault samples—gear tooth breakage, tooth corrosion, and a compound fault combining the two—were fabricated to reflect common degradation modes observed in practical wind turbine systems. Vibration signals collected under these controlled conditions were used to develop and validate a fault diagnosis model capable of accurately distinguishing different failure modes, thereby supporting reliable condition monitoring and predictive maintenance. Details of the wind turbine gearbox fault simulation platform and the fabrication of fault samples are described as follows.

2.1 Experimental platform for wind turbine gearbox

The experimental platform, shown in Fig. 1, was designed to simulate the wind energy conversion process and reproduce operational fault conditions of a wind turbine gearbox. It consists of a wind turbine blade, a three-phase induction motor, a gearbox, and a wound-rotor induction generator. The induction motor, controlled through a driver, provides the rotational input that mimics turbine blade movement. Mechanical energy is transmitted through the gearbox to increase rotational speed before being delivered to the generator for electrical power conversion. To enable real-time monitoring, a high-sensitivity triaxial vibration sensor (KS943B.100) was integrated with an NI-9234 module and cDAQ-9171 chassis to form a high-speed data acquisition system capable of capturing high-frequency vibration signals with precise timing. The collected vibration data under normal and faulty gearbox conditions were subsequently used to train and evaluate the proposed 1D-CNN-based diagnostic model.

2.2 Construction of wind turbine gearbox fault models

The internal gear components of the wind turbine gearbox were manufactured through standard machining and heat-treatment procedures, including material cutting, gear milling, quenching, tempering, and precision grinding to ensure dimensional accuracy and mechanical strength. The assembled healthy gearbox, illustrated in Fig. 2, includes four primary gears ($Gear_1$ to $Gear_4$) with corresponding tooth numbers (T_1 to T_4), and three principal shaft speeds (low-speed shaft N_{Low}, intermediate shaft N_{Low}^{High}, and high-speed shaft N_{High}), providing the baseline configuration for fault simulation. To construct representative fault models consistent with degradation mechanisms reported in Ref. 18, three typical failure conditions were intentionally induced. Gear tooth breakage was produced by mechanically removing a portion of the tooth surface using an industrial grinding machine to replicate fracture caused by overload

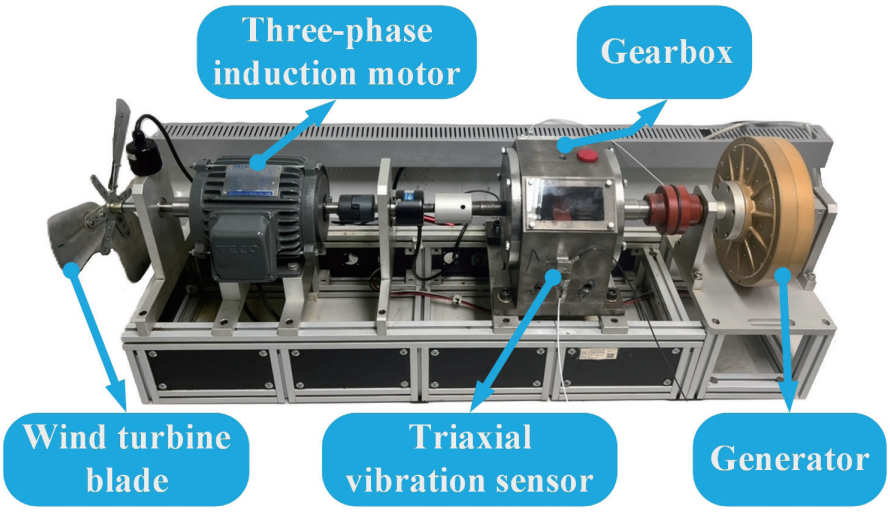

Fig. 1. (Color online) Experimental platform for wind turbine gearbox fault detection.

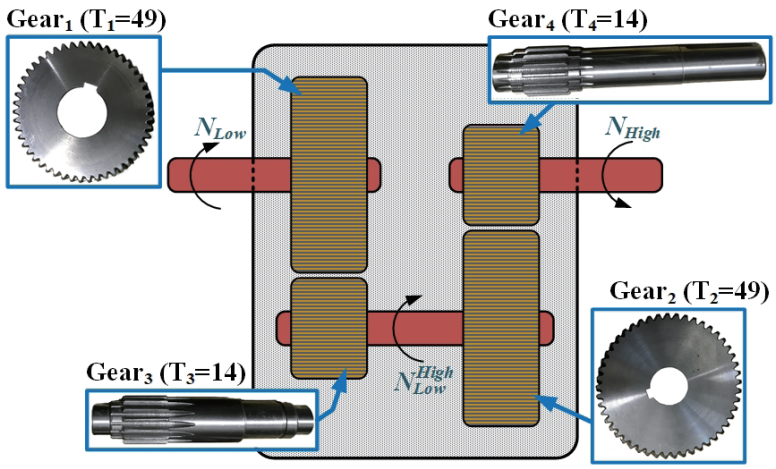

Fig. 2. (Color online) Internal gear components and structural configuration of the gearbox.

or improper assembly. Gear tooth corrosion was generated by immersing a healthy gear in industrial hydrochloric acid for 3 to 5 days, followed by air exposure to accelerate oxidation, simulating corrosion due to lubricant deterioration and prolonged operation in humid or saline environments. The compound fault model was created by sequentially applying mechanical damage and chemical corrosion to emulate the combined effects of mechanical fatigue and environmental degradation frequently observed in wind turbine gearboxes. These three fault models, shown in Fig. 3, were subsequently installed on the experimental platform to produce vibration datasets for training and evaluating the proposed fault detection method.

3. Proposed Fault Detection Method

To accurately classify and identify faults in wind turbine gearboxes, a fault detection framework based on a 1D-CNN is proposed. Owing to its end-to-end feature extraction capability, the 1D-CNN can directly process raw vibration signals without extensive preprocessing or manual feature design.[19–21] Compared with traditional statistical or frequency-domain approaches, the 1D-CNN preserves the essential temporal characteristics of the input, enhancing classification accuracy under various operating conditions and diverse fault types. This makes it particularly suitable for health monitoring in complex industrial environments.

The convolutional layers serve as the core feature extractors in the 1D-CNN. By convolving the input signal with kernels of predefined sizes, the model captures representative local temporal patterns. Kernel size is critical: excessively small kernels may miss salient features whereas overly large kernels increase computational cost and model complexity. Therefore, appropriate combinations of kernel size, stride, and padding are typically selected to ensure efficient feature extraction. The convolution operation is defined as

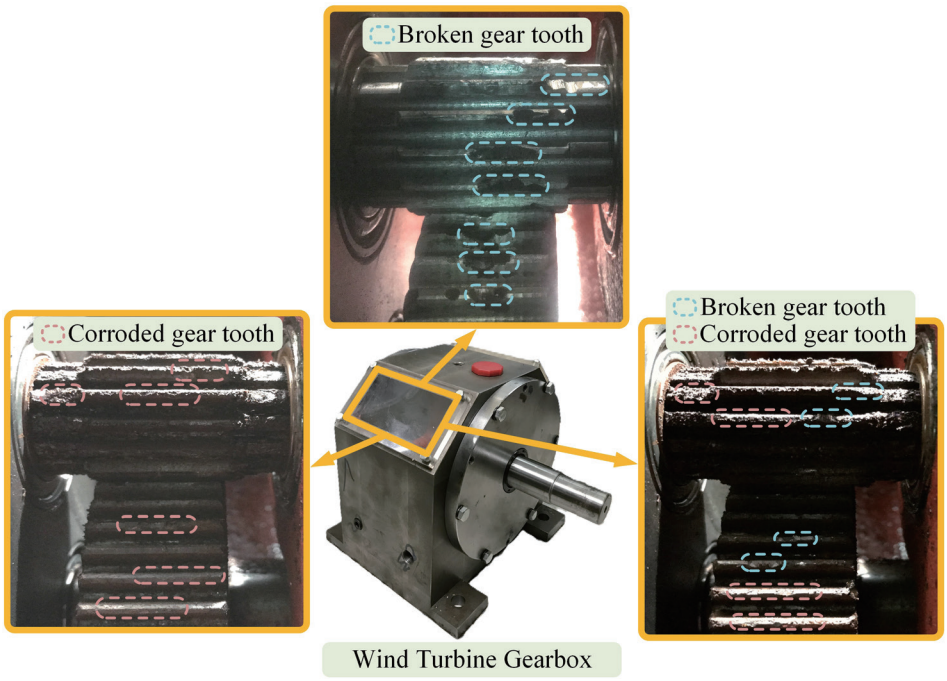

Fig. 3. (Color online) Fault models of the wind turbine gearbox.

$$S_i^{(l)} = f\left(\sum_{j=1}^{n} S_j^{(l-1)} \otimes K_{i,j}^{(l)} + b_i^{(l)}\right), \tag{1}$$

where $S_i^{(l)}$ represents the i-th output feature at the l-th layer, while $S_j^{(l-1)}$ denotes the j-th input feature from the $(l-1)$-th layer. $K_{i,j}^{(l)}$ refers to the convolutional kernel weight, and n is the number of input features. $b_i^{(l)}$ is the bias term, $f(\cdot)$ denotes the nonlinear activation function, and $\otimes$ indicates the one-dimensional convolution operation.

Activation functions introduce nonlinearity into the 1D-CNN, enabling the model to learn complex relationships beyond linear transformations.[22] Among various activation functions, the Rectified Linear Unit (ReLU) function is widely adopted owing to its computational efficiency, reduced risk of vanishing gradients, and ability to promote sparse activations.[23] It is expressed as

$$f(S_R) = \begin{cases} 0, & \text{if } S_R < 0 \\ S_R, & \text{if } S_R \geq 0 \end{cases}, \tag{2}$$

where S_R denotes the output of the convolutional layer, and the ReLU function outputs the input value directly when it is positive; otherwise, it outputs zero.

Following the convolution operation, a pooling layer is used to reduce feature map dimensionality and computational burden while retaining key information. Max pooling and

average pooling are common strategies; however, max pooling is adopted in this study as it emphasizes prominent local variations that typically correspond to fault-induced anomalies. The max-pooling process is defined as

$$S_i^{(l)} = \underset{p \in R_i}{max} S_p^{(l-1)}, \tag{3}$$

where R_i denotes the receptive field of the pooling region, $S_p^{(l-1)}$ represents the input feature values at the corresponding positions from the previous layer, and $S_i^{(l)}$ denotes the output feature value obtained through the max pooling operation.

The flatten layer transforms the multidimensional feature maps into a one-dimensional vector, forming the input to the fully connected (FC) layers. This vector aggregates the abstract features learned by previous layers and provides a standardized representation for final classification.

The FC layer performs global integration of extracted features, and its output is passed to the Softmax classifier, which converts the results into class probability distributions. The Softmax function is defined as

$$y_i = \frac{e^{z_i}}{\sum_{j=1}^{Fy} e^{z_j}}, \tag{4}$$

where y_i denotes the predicted probability for the i-th class, Fy represents the total number of classification categories, and z_j indicates the output value from the previous layer.

4. Measurement and Result Analysis

The architecture of the proposed wind turbine gearbox fault detection system is shown in Fig. 4. A triaxial accelerometer mounted on the gearbox acquires raw vibration signals along the *X*, *Y*, and *Z* axes at a fixed sampling rate, ensuring signal continuity and integrity for subsequent analysis. Unlike conventional fault diagnosis approaches that rely on manual feature extraction or frequency-domain transformations, the proposed method directly inputs raw time-domain vibration signals into a custom-designed 1D-CNN. By leveraging hierarchical convolutional and pooling operations, the model autonomously learns representative features without the need for handcrafted feature engineering, thereby simplifying the diagnostic pipeline while improving accuracy, robustness, and practical applicability.

4.1 Measurement of raw vibration signals from wind turbine gearbox

Diagnostic experiments were conducted under three common gearbox fault conditions in wind turbines: gear tooth breakage, tooth corrosion, and a combined fault involving the two mechanisms. Triaxial vibration signals were measured at a sampling rate of 12.8 kS/s, producing

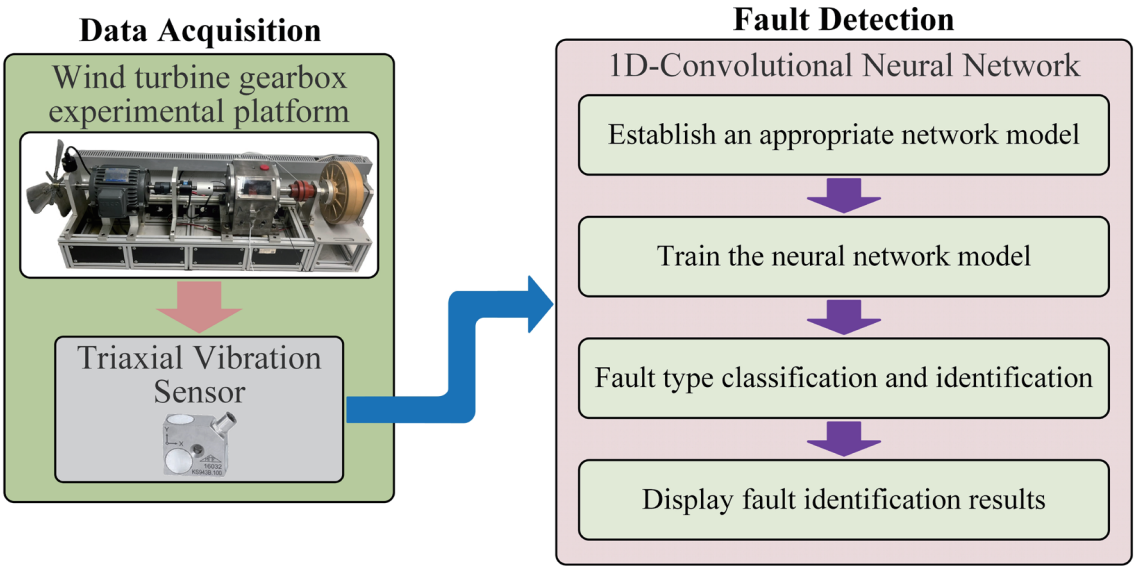

Fig. 4. (Color online) System architecture of the proposed gearbox fault detection method.

12800 data points per record, which provides sufficient temporal resolution for capturing subtle fault-related signatures. For each fault type, 500 triaxial vibration samples were collected; among them, 400 samples were randomly selected for training the 1D-CNN, while the remaining 100 samples were retained for testing. The raw vibration waveforms under different fault conditions are shown in Fig. 5. As illustrated, the time-domain signals exhibit similar patterns across fault categories, making traditional waveform-based identification highly challenging. By contrast, the 1D-CNN effectively exploits local feature extraction, parameter sharing, and translation invariance to autonomously learn discriminative representations from raw signals. This capability significantly enhances detection accuracy and robustness, demonstrating the feasibility and practical effectiveness of the proposed approach for real-world wind turbine gearbox fault diagnosis.

4.2 Detection results of the proposed method

To implement the proposed fault detection system, the 1D-CNN algorithm was developed using MATLAB 2020b and executed on a workstation equipped with an Intel® Core™ i7-9700 CPU, an NVIDIA RTX 2080 SUPER GPU, and a 64-bit Windows 10 operating system. The network architecture, shown in Fig. 6, consists of three convolutional layers, three max-pooling layers, a flatten layer, and a fully connected layer with a Softmax classifier. The model receives triaxial vibration signals with an input dimension of 12800 × 3. All three convolutional layers employ 64 filters with a kernel size of 9 applied along the temporal axis to extract representative temporal features. ReLU activation functions are applied after each convolutional layer, and batch normalization is incorporated to stabilize training and enhance convergence without the use of dropout. Each convolutional block is followed by a max pooling layer with a pooling size of 2, which reduces the dimensionality of the feature maps while preserving salient temporal

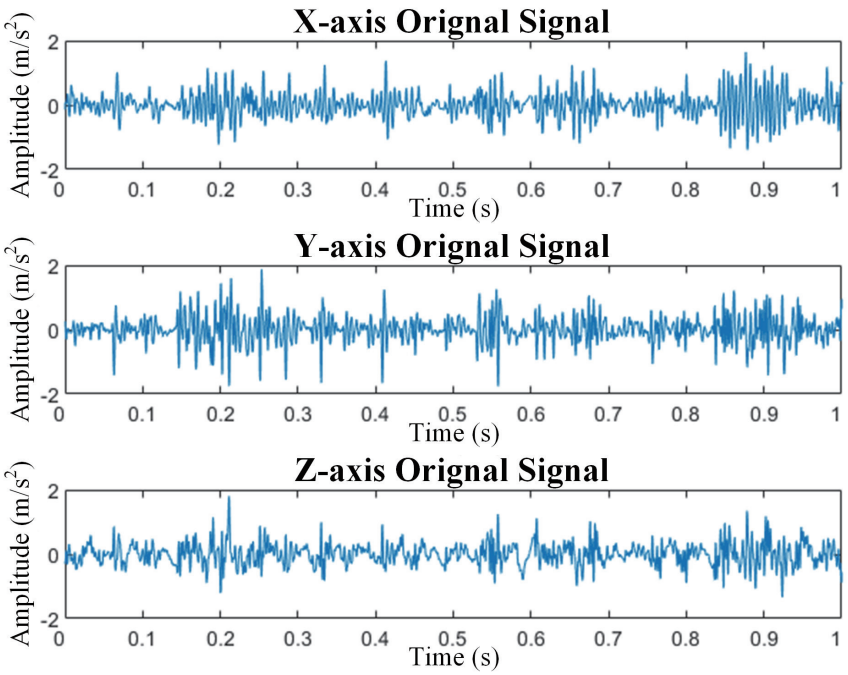

Fig. 5. (Color online) Time-domain waveforms of triaxial vibration signals from the wind turbine gearbox.

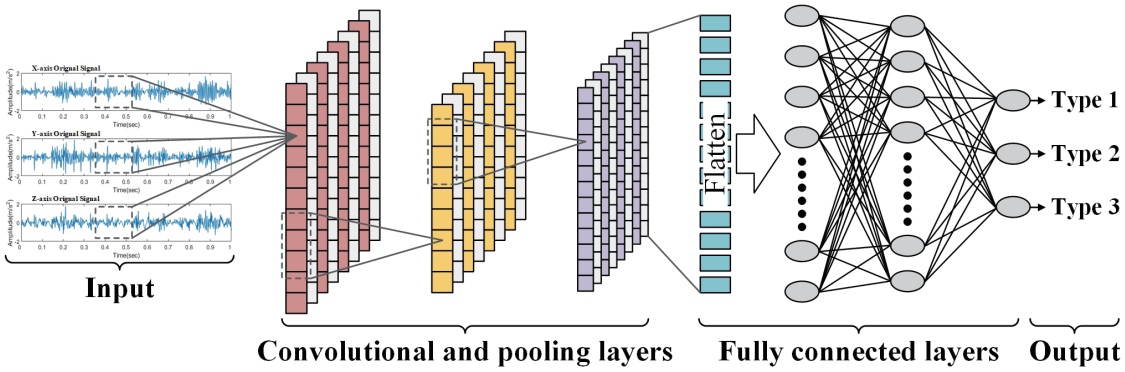

Fig. 6. (Color online) Architecture of the 1D-CNN.

characteristics. The resulting feature maps are then flattened and passed to a fully connected layer with a Softmax classifier for the final fault-type prediction. Key architectural elements—including kernel size, number of filters, activation function, and pooling strategy—were systematically evaluated to determine the optimal configuration, resulting in a model that achieves both high accuracy and computational efficiency. The hyperparameters used during the training phase of the 1D-CNN are detailed in Table 1.

A total of 1200 triaxial vibration samples (400 per fault type: tooth breakage, corrosion, and compound fault) were used for model training. To evaluate the generalization capability and detection performance, an additional set of 300 unseen samples (100 per fault type) was reserved for testing. The proposed 1D-CNN achieved a fault classification accuracy of 98.7%,

Table 1
Hyperparameter settings for 1D-CNN training.

Hyperparameter option	Set value
Solver for training network (solverName)	adam
Hardware resource for training network (ExecutionEnvironment)	GPU
Initial learning rate (InitialLearnRate)	0.0375
Maximum number of epochs (MaxEpochs)	50
Size of minibatch (MiniBatchSize)	10
Frequency of network validation (ValidationFrequency)	50
Option for data shuffling (Shuffle)	every-epoch
Data for validation during training (ValidationData)	Same data type as training data

demonstrating strong robustness and reliable discrimination among different gearbox fault states. The confusion matrix in Fig. 7 summarizes the classification outcomes, where the *x*-axis and *y*-axis indicate predicted and actual classes, respectively. Green cells represent correct classifications, red cells denote misclassifications, and the per-class accuracy and error rates are provided along the matrix margins. The bottom-right cell displays the overall classification performance, confirming the effectiveness of the proposed approach.

The computational performance of the model was further evaluated under the same hardware environment. The trained 1D-CNN achieves an average inference latency of 267.19 ms per sample, supporting near real-time detection, while the complete training process requires only 19.28 min, demonstrating efficient model development without heavy computational demands. These results confirm that the proposed 1D-CNN delivers high diagnostic accuracy together with a practical computational performance suitable for real-world wind turbine gearbox monitoring applications.

4.3 Comparative analysis with other detection methods

In this study, a chaos synchronization detection technique was employed to convert triaxial vibration signals into chaotic dynamic error scatter plots for benchmarking the proposed 1D-CNN against several alternative fault detection approaches, including a 2D-CNN model and HOG-based feature extraction combined with SVM, BPNN, and KNN classifiers. As summarized in Table 2, the proposed 1D-CNN demonstrates clear performance advantages across all evaluation metrics. It achieves the highest accuracy, precision, recall, and F1-score (all 98.7%), outperforming the 2D-CNN model, whose accuracies range from 97 to 98%, and significantly surpasses the HOG-based methods, which achieve lower performance with accuracies of 85.3–87.7% (SVM), 95.7–97.3% (BPNN), and 85.7–87% (KNN). Detection efficiency further highlights the superiority of the proposed method: its detection time of 0.0029 s is shorter than that of the 2D-CNN (0.0036 s) and all HOG-based classifiers (0.0058–0.0087 s). This improvement results from the 1D-CNN's ability to process raw time-domain signals directly without image conversion or manual feature extraction, thereby avoiding unnecessary computational overhead and potential information loss. Additionally, the integration of all three vibration axes enables the model to capture a more comprehensive representation of gearbox dynamics, leading to enhanced robustness and fault discrimination capability. To ensure

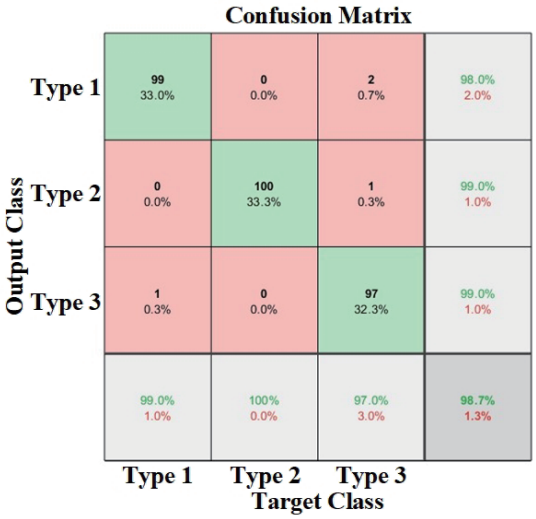

Fig. 7. (Color online) Confusion matrix of wind turbine gearbox fault detection results.

Table 2
Results of different fault detection methods.

Detection method	Input signals	Detection time (s)	Accuracy (%)	Precision (%)	Recall (%)	F1-score (%)
1D-CNN	Triaxial vibration	0.0029	98.7	98.7	98.7	98.7
2D-CNN	*X*-axis vibration	0.0036	97	97	97	97
	Y-axis vibration		97.7	97.7	97.7	97.7
	Z-axis vibration		98	98	98	98
HOG+SVM	*X*-axis vibration	0.0058	85.3	85.3	85.3	85.3
	Y-axis vibration		87	87	87	87
	Z-axis vibration		87.7	87.7	87.7	87.7
HOG+BPNN	*X*-axis vibration	0.0073	95.7	95.7	95.7	95.7
	Y-axis vibration		96.3	96.3	96.3	96.3
	Z-axis vibration		97.3	97.3	97.3	97.3
HOG+KNN	*X*-axis vibration	0.0087	85.7	85.7	85.7	85.7
	Y-axis vibration		86.3	86.3	86.3	86.3
	Z-axis vibration		87	87	87	87

statistical reliability, all methods were evaluated over five independent trials with different random initializations, and the reported performance represents the average results across these trials. The consistent outcomes verify that the proposed 1D-CNN provides superior accuracy, faster detection speed, and more stable performance, demonstrating strong potential for real-time fault diagnosis in wind turbine gearboxes.

5. Conclusions

A fault detection method for wind turbine gearboxes based on one-dimensional convolutional neural network (1D-CNN), which directly processes raw triaxial time-domain vibration signals was proposed. By eliminating the need for traditional feature engineering and image transformation procedures, the proposed approach significantly enhances both classification accuracy and real-time performance. Three common gearbox fault types, namely, gear tooth

breakage, gear tooth corrosion, and combined tooth breakage with corrosion, were constructed, and corresponding triaxial vibration signals were collected for model training and testing. Experimental results demonstrated that the proposed 1D-CNN method achieves a fault classification accuracy of up to 98.7%, outperforming conventional approaches that utilize HOG features in conjunction with SVM, BPNN, and KNN classifiers, as well as image-based 2D-CNN detection methods. Moreover, the 1D-CNN model exhibits the shortest processing time among the compared methods, confirming its potential for high-precision and real-time fault diagnosis applications. This work not only demonstrates the practical applicability of 1D-CNN for monitoring the operational condition of wind turbine gearboxes, but also provides a viable framework for general mechanical fault detection. Future efforts may further extend the model to accommodate more complex operating conditions and integrate multisource sensor data to enhance generalization capability and adaptability, ultimately enabling more efficient and robust predictive maintenance systems.

References

1 P. Kayal and C. K. Chanda: Renewable Energy **75** (2015) 173. https://doi.org/10.1016/j.renene.2014.10.003
2 R. S. Amano: ASME. J. Energy Res. Technol. **139** (2017) 050801. https://doi.org/10.1115/1.4037757
3 J. M. Ha and O. Fink: Mech. Syst. Signal Process. **202** (2023) 110680. https://doi.org/10.1016/j.ymssp.2023.110680
4 A. Amin, A. Bibo, M. Panyam, and P. Tallapragada: Wind Eng. **47** (2022) 175. https://doi.org/10.1177/0309524X221123968
5 Z. Liu and L. Zhang: Measurement **149** (2020) 107002. https://doi.org/10.1016/j.measurement.2019.107002
6 S. Asgari and A. Yazdizadeh: Energy Syst. **9** (2018) 921. https://doi.org/10.1007/s12667-017-0231-2
7 M. Li, D. Yu, Z. Chen, K. Xiahou, T. Ji, and Q. H. Wu: IEEE Trans. Sustainable Energy **10** (2019) 895. https://doi.org/10.1109/TSTE.2018.2853990
8 J. H. Zhong, J. Zhang, J. Liang, and H. Wang: IEEE Access **7** (2019) 773. https://doi.org/10.1109/ACCESS.2018.2885816
9 Z. Pu, C. Li, S. Zhang, and Y. Bai: IEEE Trans. Instrum. Meas. **70** (2021) 1. https://doi.org/10.1109/TIM.2020.3024048
10 Q. He, J. Zhao, G. Jiang, and P. Xie: IEEE Trans. Instrum. Meas. **69** (2020) 5569. https://doi.org/10.1109/TIM.2020.2964064
11 X. Xia, X. Wang, and W. Chen: Entropy **27** (2025) 192. https://doi.org/10.3390/e27020192
12 P. Trizoglou, X. Liu, and Z. Lin: Renewable Energy **179** (2021) 945. https://doi.org/10.1016/j.renene.2021.07.085
13 J. Yang, S. Yin, Y. Chang, and T. Gao: Sensors **20** (2020) 3837. https://doi.org/10.3390/s20143837
14 C. C. Chen, Z. Liu, G. Yang, C. C. Wu, and Q. Ye: Electronics **10** (2021) 59. https://doi.org/10.3390/electronics10010059
15 C. Du, R. Zhong, Y. Zhuo, X. Zhang, F. Yu, F. Li, Y. Rong, and Y. Gong: Eng. Res. Express **4** (2022) 015003. https://doi.org/10.1088/2631-8695/ac4834
16 T. Xie, W. Zhang, Y. Zhang, Z. Ahmed, and Y. Tang: IEEE Trans. Instrum. Meas. **72** (2023) 1. https://doi.org/10.1109/TIM.2023.3267342
17 B. L. Jian, C. C. Wang, J. Y. Chang, X. Y. Su, and H. T. Yau: IEEE Access **7** (2019) 67278. https://doi.org/10.1109/ACCESS.2019.2917094
18 A. Kumar, C.P. Gandhi, Y. Zhou, R. Kumar, and J. Xiang: Measurement **158** (2020) 107735. https://doi.org/10.1016/j.measurement.2020.107735
19 H. Habbouche, Y. Amirat, T. Benkedjouh, and M. Benbouzid: IEEE Trans. Energy Convers. **37** (2022) 466. https://doi.org/10.1109/TEC.2021.3085909
20 Y. Chen and L. Xiao: IEEE Sens. J. **24** (2024) 3406. https://doi.org/10.1109/JSEN.2023.3342891
21 C. Li, J. Xu, and J. Xing: IEEE Sens. J. **24** (2024) 564. https://doi.org/10.1109/JSEN.2023.3334037
22 Z. Li, F. Liu, W. Yang, S. Peng, and J. Zhou: IEEE Trans. Neural Networks Learn. Syst. **33** (2022) 6999. https://doi.org/10.1109/TNNLS.2021.3084827
23 R. Magar, L. Ghule, J. Li, Y. Zhao, and A. B. Farimani: IEEE Access **9** (2021) 25189. https://doi.org/10.1109/ACCESS.2021.3056944

About the Authors

Hong-Wei Sian received his M.S. degree in electrical engineering from National Changhua University of Education (NCUE), Changhua City, Taiwan, in 2006, and his Ph.D. degree in electrical engineering from National Taiwan University of Science and Technology (NTUST), Taipei City, Taiwan, in 2024. He is currently an assistant professor in the Department of Electrical Engineering, National Chin-Yi University of Technology, Taichung City, Taiwan. His research interests include equipment fault diagnosis, renewable energy systems, programmable logic controller, and automation control application. (hwsian@ncut.edu.tw)